

Spin arrangement diagrams for $\text{Er}_{2-x}\text{R}_x\text{Fe}_{14}\text{B}$ ($\text{R} = \text{Y}, \text{Ce}$) obtained with Mössbauer spectroscopy and phenomenological model

Antoni T. Pędziwiatr,
Bogdan F. Bogacz,
Renata Gargula

Abstract Two isostructural series of polycrystalline compounds: $\text{Er}_{2-x}\text{Y}_x\text{Fe}_{14}\text{B}$ and $\text{Er}_{2-x}\text{Ce}_x\text{Fe}_{14}\text{B}$ have been studied by ^{57}Fe Mössbauer spectroscopy in the temperature range 80–370 K. The spin reorientation phenomenon (a transition from basal plane to axial easy magnetisation direction) has been studied extensively by a narrow step temperature scanning in the vicinity of the transition. Using the procedure of subtracting the Mössbauer spectra taken for the same compound at different temperatures, it was possible to follow the influence of transition on the shape of spectra. From this procedure it was concluded that in the region of transition each subspectrum splits into two Zeeman sextets, which are characterised by different hyperfine magnetic fields and quadrupole splittings. The consistent way of describing the Mössbauer spectra was proposed. The spin reorientation temperatures have been established for all compositions and compared with the values obtained from theoretical calculations of spin orientation angle based on phenomenological model. The spin arrangement diagrams have been constructed.

Key words Mössbauer effect • permanent magnet materials • spin diagrams • spin reorientation

Introduction

The Er-based $\text{R}_2\text{Fe}_{14}\text{B}$ ($\text{R} = \text{rare earth}$) intermetallics exhibit many interesting magnetic properties including spin reorientation phenomena. $\text{Er}_2\text{Fe}_{14}\text{B}$ changes its spin arrangement at the spin reorientation temperature, T_{SR} , of 324 K. Up to now, several groups [4–6, 11, 14, 15, 17] have studied the nature of spin reorientation phenomena in yttrium substituted $\text{Er}_{2-x}\text{Y}_x\text{Fe}_{14}\text{B}$ and cerium substituted $\text{Er}_{2-x}\text{Ce}_x\text{Fe}_{14}\text{B}$ compounds trying to establish the influence of substituents on the Er sublattice anisotropy.

In these compounds, the macroscopic anisotropy changes from planar (spin orientation angle with respect to crystallographic c -axis, $\theta = 90^\circ$) to axial (along c -axis, $\theta = 0^\circ$) with increasing temperature. The actual easy magnetisation direction of $\text{Er}_{2-x}\text{R}_x\text{Fe}_{14}\text{B}$ depends on temperature induced competition between the uniaxial Fe sublattice anisotropy [8] and the basal plane (Er, R) sublattice anisotropy [10].

The $\text{Er}_{2-x}\text{R}_x\text{Fe}_{14}\text{B}$ ($\text{R} = \text{Y}, \text{Ce}$) intermetallic compounds crystallise in a tetragonal structure with space group $\text{P4}_2/\text{mnm}$ [9]. Iron atoms occupy six non-equivalent crystal sites ($16k_1$, $16k_2$, $8j_1$, $8j_2$, $4e$, $4c$), the rare earth ions occupy $4f$ and $4g$ crystallographic sites and boron is located at $4g$ site. Recent study by single crystal neutron diffraction on $\text{Er}_2\text{Fe}_{14}\text{B}$ [18] revealed that there is a change of crystal structure to orthorhombic below the spin reorientation transition.

In this study, the polycrystalline $\text{Er}_{2-x}\text{Y}_x\text{Fe}_{14}\text{B}$ ($x = 0.0, 0.5, 1.0, 1.5$) and $\text{Er}_{2-x}\text{Ce}_x\text{Fe}_{14}\text{B}$ ($x = 0.25, 0.5, 1.0$) isostructural compounds have been investigated by ^{57}Fe Mössbauer spectroscopy using a narrow step temperature scanning in order to establish the spin reorientation temperatures, to determine the temperature region of spin

A. T. Pędziwiatr[✉], B. F. Bogacz, R. Gargula
Marian Smoluchowski Institute of Physics,
Jagiellonian University,
4 Reymonta, 30-059 Kraków, Poland,
Tel.: +48 12/ 632 48 88, Fax: +48 12/ 633 70 86,
e-mail: ufpedziw@if.uj.edu.pl

Received: 17 July 2002, Accepted: 17 September 2002

reorientation and the influence of reorientation on hyperfine interaction parameters. Our goal was also to propose a consistent description of Mössbauer spectra in the whole range of temperatures and to construct spin arrangement diagrams for the two series, as well as to compare the experimental results with theoretical calculations based on the phenomenological model of Yamada-Kato [19].

Experimental details

The $\text{Er}_{2-x}\text{R}_x\text{Fe}_{14}\text{B}$ ($\text{R} = \text{Y}, \text{Ce}$) materials were obtained by a standard procedure of the induction melting under flowing high purity argon and the subsequent annealing at 900°C for two weeks. The X-ray and thermomagnetic analysis proved the single phase integrity of materials. However, the Mössbauer spectra, taken using a $^{57}\text{Co}(\text{Rh})$ source and a computer driven constant acceleration mode spectrometer, indicated a small amount of natural iron impurity in $\text{Er}_2\text{Fe}_{14}\text{B}$ (about 2%) and in $\text{ErYFe}_{14}\text{B}$ (about 1%). These small impurity patterns were subtracted from the experimental spectra by the numerical procedure. The ^{57}Fe Mössbauer transmission spectra were recorded in the temperature range 80–340 K. The spin reorientation phenomenon near T_{SR} has been studied extensively by a narrow step (sometimes 1 K) temperature scanning. A high purity iron foil was used to calibrate the velocity scale. Isomer shifts were established with respect to the centre of gravity of the room temperature iron Mössbauer spectrum.

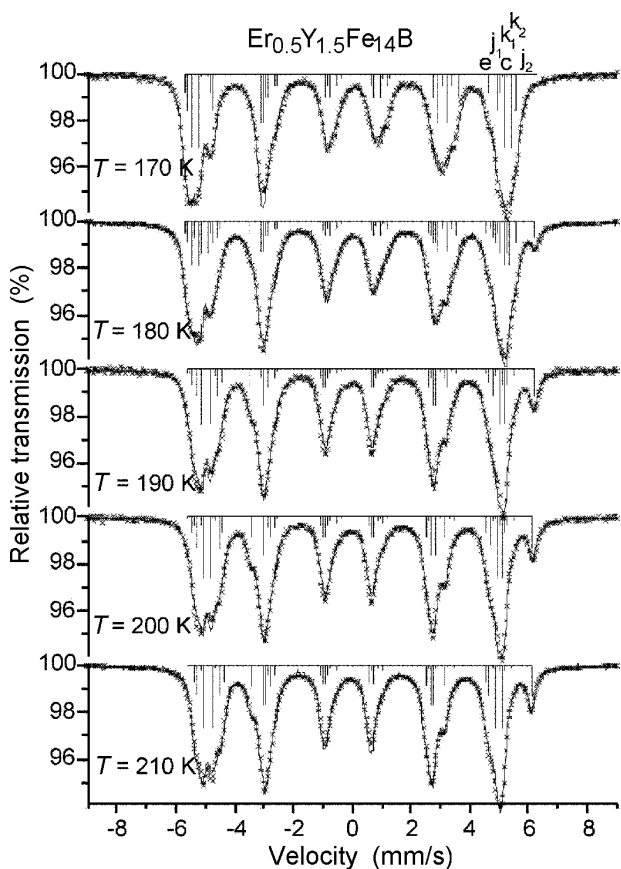


Fig. 1. The selected ^{57}Fe Mössbauer transmission spectra for the $\text{Er}_{2-x}\text{Y}_x\text{Fe}_{14}\text{B}$ ($x = 1.5$) intermetallic compound. The solid lines are fits to the data. The stick diagrams show the line positions and relative intensities.

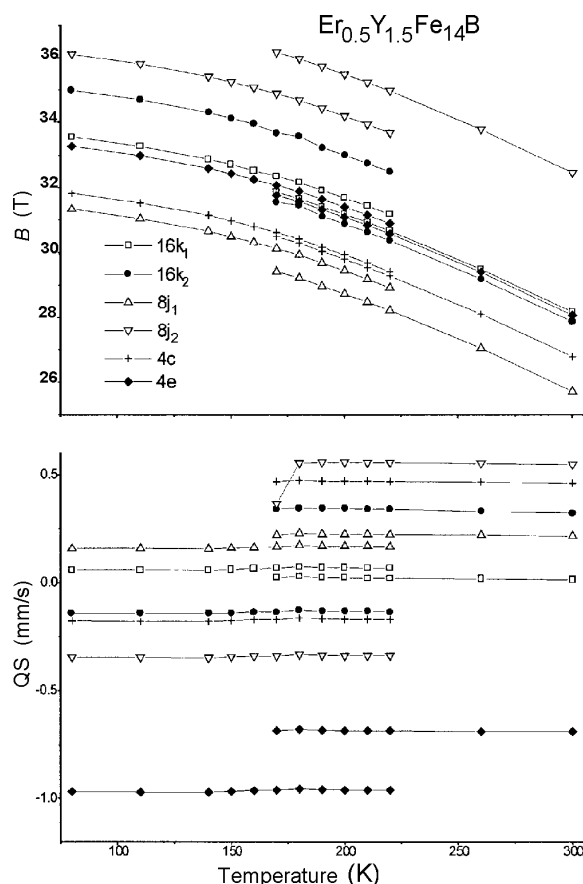


Fig. 2. Temperature dependencies of the hyperfine magnetic field (B), and quadrupole splitting (QS) for different crystal sites of $\text{Er}_{0.5}\text{Y}_{1.5}\text{Fe}_{14}\text{B}$. The average error is 0.01 mm/s. The dual assignment in the spin reorientation region is connected with coexistence of “low” and “high temperature” sextets.

Data analysis

The “exponential” approximation [2] of the transmission integral was used to describe the investigated Mössbauer spectra, similarly as in [17]. A simultaneous constrained fitting of several Mössbauer spectra gave opportunity to establish consistently the temperature dependence of hyperfine interaction parameters. The spectra below and above the temperature region of spin reorientation, were analysed using six Zeeman subspectra with relative intensities according to iron occupation of crystallographic sublattices (4:4:2:2:1:1). Each subspectrum was characterised by following hyperfine interaction parameters: magnetic field, B ; isomer shift, IS; quadrupole splitting, QS (defined as $[(V_6 - V_5) - (V_2 - V_1)]/2$ where V_i are velocities corresponding to Mössbauer line positions). The experimental Mössbauer spectra of $\text{Er}_{0.5}\text{Y}_{1.5}\text{Fe}_{14}\text{B}$ compound for selected temperatures are shown in Fig. 1 as an example of spectra obtained for the two series of the studied compounds.

Due to systematic difficulties in describing the experimental Mössbauer spectra in the transition region, we used the procedure which allowed us to observe direct changes in the shape of Mössbauer spectra: two spectra of the same compound recorded at different temperatures were numerically subtracted [12, 13]. The procedure of subtraction was preceded by the correction of the subtracted spectrum which took into consideration the

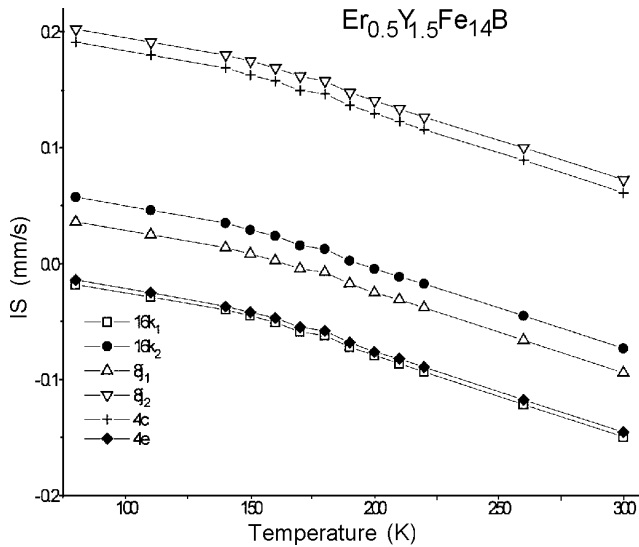


Fig. 3. The temperature dependence of IS for different crystal sites of $\text{Er}_{0.5}\text{Y}_{1.5}\text{Fe}_{14}\text{B}$. The average error is 0.01 mm/s.

temperature changes of IS and B . Values of changes per 1 K ($\Delta\text{IS}/\Delta T$, $\Delta B/\Delta T$) were determined on the basis of the analysis of Mössbauer spectra recorded beyond the spin reorientation region. The subtraction of spectra recorded at a narrow step temperature interval allowed us to observe relatively sudden changes connected with spin reorientation. The analysis presented above shows the temperature range of the reorientation process and suggests that all sublattices take part in the spin reorientation collectively.

The following idea of description of the experimental Mössbauer spectra was used: spectra below spin reorientation region were described by “low temperature” Zeeman sextets and above – by “high temperature” Zeeman sextets. There is a coexistence of the “low” and “high temperature” Zeeman sextets in the region of the transition. Both kinds of Zeeman sextets exchange gradually (between themselves) their contributions C_l , C_h to the total spectrum and have different values of B and QS. The weak, systematic changes of B and QS with temperature were taken into account for spectra below and above spin reorientation region (Fig. 2). A common linear temperature dependence of IS caused by second order Doppler shift effect was assumed for “low” and “high temperature” Zeeman sextets (Fig. 3). This description is similar to the procedure applied for polycrystalline $\text{Er}_2\text{Fe}_{14}\text{B}$ [19]. Figs. 2 and 3 show examples of temperature dependence of hyperfine parameters assigned to six sublattices obtained from fits [12, 13]. A smooth and continuous character of change as well as fit quality parameters indicate the consistency of fits throughout the series.

Table 1. Crystal and exchange field parameters (in Kelvin) for $\text{R}_2\text{Fe}_{14}\text{B}$ (R = Er, Ce) compounds. The same parameters for f and g sites are taken from [19] for Er and Ce from ** [16] and * calculated by using the crystal field coefficients for Nd [19] and B_n^m/A_n^m relations for Ce [7].

R	B_2^0	B_2^2	B_4^0	B_4^4	B_6^0	B_6^4	$2(g_s-1)B_{\text{ex}}$
Er	0.455	-0.848	0.72×10^{-3}	0.0	-0.98×10^{-5}	-5.31×10^{-5}	58
Ce	-21.1**	34.0*	-0.31*	0.0	0.0	0.0	39**

One of our goals was to find the temperature range of the spin reorientation phenomenon and to determine the spin reorientation temperature using the Mössbauer method. The most useful feature which enables to do this is the separation of the sixth line in the $8j_2$ high temperature subspectrum of the analysed experimental spectra. Owing to the clear development of its intensity in the course of the transition, it was possible to establish precisely the contributions of “high-”, C_h , and “low temperature”, $C_l = 1 - C_h$, Zeeman sextets to the spectrum and conclude on the spin reorientation temperature.

Phenomenological model

The simplified Yamada-Kato model [3, 19] was used to describe the temperature and composition dependence of spin reorientation in the $\text{R}_2\text{Fe}_{14}\text{B}$ compounds. The angle of spin orientation was determined by minimising the free energy, $F(T, \theta)$. The free energy of the system is assumed to be the sum of contributions from the R- and the Fe-sublattices

$$(1) \quad F(T) = F_{\text{R}}(T) + F_{\text{Fe}}(T).$$

The R-sublattice is treated as an assembly of isolated atoms (R-R interaction is neglected) in the crystal electric field (CEF) and exchange field which describe the R-Fe interaction. Contribution to the free energy is calculated from a single ion Hamiltonian. The CEF and exchange field parameters needed for calculations are taken from the literature (Table 1). The contributions from different R ions were assumed to be linear.

For the Fe sublattice the free energy is approximated by anisotropy energy (it is expected that the entropy term is negligible). Anisotropy energy is introduced in a phenomenological way, based on the temperature dependence of anisotropy constant $K_1(T)$ obtained experimentally [1] and scaled in temperatures to the Curie temperature of each compound.

The total free energy is given by the formula [19]

$$(2) \quad F(T, \theta) = -kT \sum_{i=1}^4 \ln Z(i) + 28K_1(T) \sin^2 \theta$$

where $Z(i)$ is the partition function

$$(3) \quad Z(i) = \sum_{j=1}^{2J+1} \exp \left[-\frac{E_j(i)}{kT} \right]$$

$E_j(i)$ are the energy levels of R-ion in $i = 4f, 4g$ lattice sites.

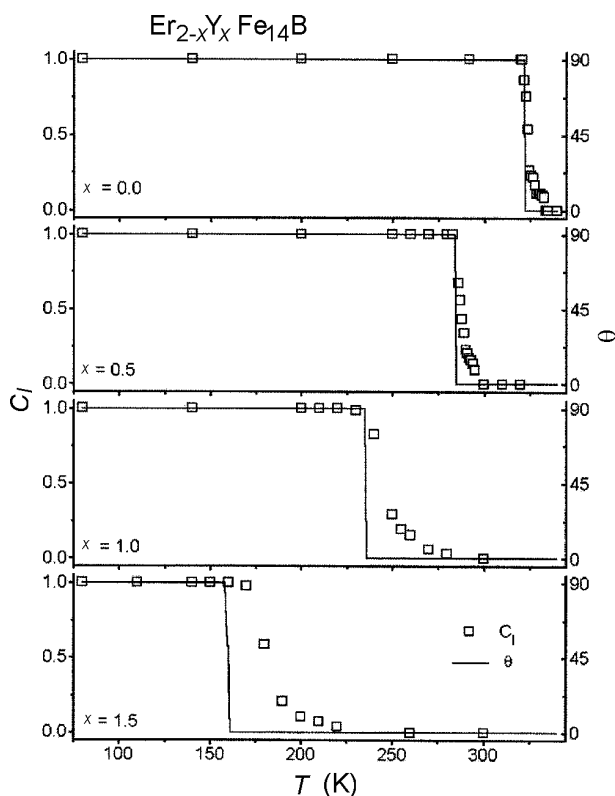


Fig. 4. Temperature dependencies of the “low temperature” Zeeman sextets contributions, C_l for $\text{Er}_{2-x}\text{Y}_x\text{Fe}_{14}\text{B}$ series. The average error is 0.02. The solid line represents the angle θ of spin orientation obtained from the theoretical model.

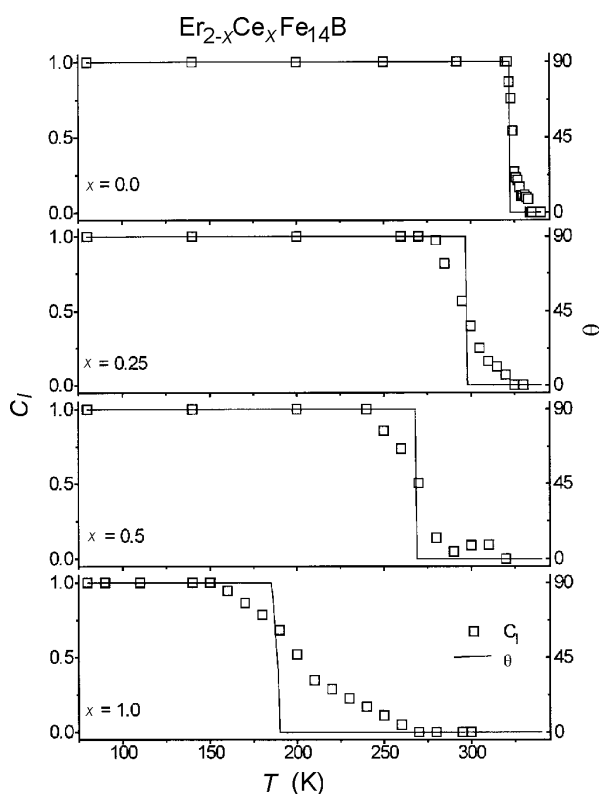


Fig. 5. Temperature dependencies of the “low temperature” Zeeman sextets contributions, C_l for $\text{Er}_{2-x}\text{Ce}_x\text{Fe}_{14}\text{B}$ series. The average error is 0.02. The solid line represents the angle θ of spin orientation obtained from the theoretical model.

Results and discussion

The experimental results of the temperature dependence of the “low temperature” contribution to Mössbauer spectra, C_l (related to planar arrangement of spins, $\theta = 90^\circ$) for Y and Ce substituted compounds are shown in Figs. 4 and 5, respectively. The change of spin orientation angle, calculated by using the described model, follows the experimentally obtained temperatures of spin reorientations, T_{SR} for all compositions.

The theoretically described process of reorientation has a typical character for the first order phase transition. For most compositions the temperature range of this process, ΔT , is less than 1 K. Only for compositions with large amounts of Y and Ce this range covers several Kelvin (for $\text{Er}_{0.5}\text{Y}_{1.5}\text{Fe}_{14}\text{B}$ $\Delta T \approx 3$ K, for $\text{ErCeFe}_{14}\text{B}$ $\Delta T \approx 5$ K).

The temperature range of the reorientation process seen by the Mössbauer method is much wider than theoretically predicted. There is a change from $\Delta T \approx 10$ K for $\text{Er}_2\text{Fe}_{14}\text{B}$ to $\Delta T \approx 90$ K for $\text{ErCeFe}_{14}\text{B}$. The behaviour of QS can give some information in trying to understand this matter. QS remains practically unchanged (and so does the spin orientation angle) in the reorientation process both for “low” and “high” temperature sextets (Fig. 2). This is seen also in Fig. 1 where the relative position of the sixth

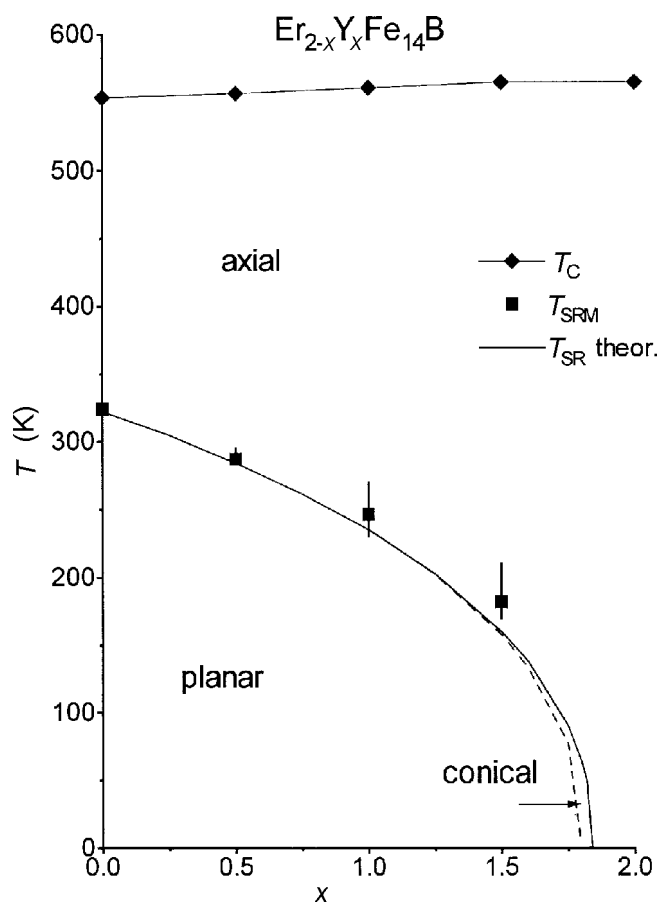


Fig. 6. Spin arrangement diagram for $\text{Er}_{2-x}\text{Y}_x\text{Fe}_{14}\text{B}$ system. T_C – Curie temperature, T_{SRM} – spin reorientation temperature determined from Mössbauer measurements. The vertical lines show the temperature range of the reorientation process. The solid and dashed lines represent the theoretically obtained limits of the range of the reorientation process. Between these lines the angle of spin orientation is $0^\circ < \theta < 90^\circ$.

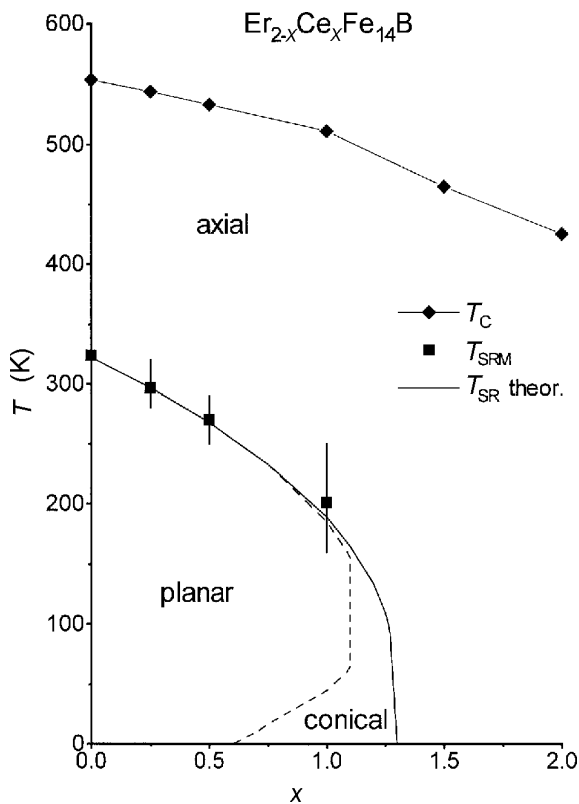


Fig. 7. Spin arrangement diagram for the $\text{Er}_{2-x}\text{Ce}_x\text{Fe}_{14}\text{B}$ system. T_C – Curie temperature, T_{SRM} – spin reorientation temperature determined from Mössbauer measurements. The vertical lines show the temperature range of the reorientation process. The solid and dashed lines represent the theoretically obtained limits of the range of the reorientation process. Between these lines the angle of spin orientation is $0^\circ < \theta < 90^\circ$.

line in $8j_2$ sextet remains unchanged. This may confirm a suggestion that the reorientation process is abrupt (typical for first order phase transition) and there are no “conical” arrangements of spins. With increasing temperature more and more spins change abruptly their position from planar to axial. The fact that this process is not observed for all the spins at the same temperature is probably due to polycrystallinity of the samples and their local microscopic inhomogeneities.

Figs. 6 and 7 show the combined spin phase diagrams for the studied compounds, indicating three different types of spin configurations: axial ($\theta = 0^\circ$), planar ($\theta = 90^\circ$) and conical ($0^\circ < \theta < 90^\circ$). The vertical lines connected with experimental points show the described above and experimentally observed temperature range of reorientation process. Theoretical lines (solid and dashed) limit the area of the conical spin arrangement. The temperature range of this arrangement for compositions related to our samples are very narrow but the agreement between the experimental and theoretical description enables to postulate the existence of conical spin arrangement for high Y(Ce) content, however it awaits experimental verification.

References

1. Andreev AV, Bartashevich MI, Goto T, Zadvorkin SM (1997) Magnetic properties of $(\text{Y}_{1-x}\text{Th}_x)_2\text{Fe}_{14}\text{B}$. *J Alloys Compd* 262/263:467–470
2. Bogacz BF (2000) On the approximation of the Mössbauer integrals. *Molecular Physics Reports* 30:15–20
3. Bogacz BF, Rubin J, Pędziwiatr AT, Bartolomé J, Wielgosz R, Artigas M (1999) Calculated and experimental magnetic phase diagrams for $(\text{Nd}, \text{Y})_2(\text{Fe}, \text{Ce})_{14}\text{B}$ systems. In: *Proc of XXXIV Zakopane School of Physics, Zakopane 1:191–198*
4. Burzo E (1998) Permanent magnets based on R-Fe-B and R-Fe-C alloys. *Rep Prog Phys* 61:1099–1266
5. Buschow KHJ (1988) Permanent magnet materials based on 3d-rich ternary compounds. In: Wohlfarth EP, Buschow KHJ (eds) *Ferromagnetic materials*, vol. 4. Elsevier, Amsterdam, pp 1–129
6. Buschow KHJ (1991) New developments in hard magnetic materials. *Rep Prog Phys* 54:1123–1213
7. Coey JMD (1996) Rare-earth iron permanent magnet. Clarendon Press, Oxford
8. Givord G, Li HS, Perrier de la Bathie R (1984) Magnetic properties of $\text{Y}_2\text{Fe}_{14}\text{B}$ and $\text{Nd}_2\text{Fe}_{14}\text{B}$ single crystals. *Solid State Commun* 51:857–860
9. Herbst JF, Croat JJ, Pinkerton FE, Yelon WB (1984) Relationships between crystal structure and magnetic properties in $\text{Nd}_2\text{Fe}_{14}\text{B}$. *Phys Rev B* 29:4176–4178
10. Hirosawa S, Matsuura Y, Yamamoto H, Fujimura S, Sagawa M, Yamauchi H (1985) Magnetization and magnetic anisotropy of $\text{R}_2\text{Fe}_{14}\text{B}$ measured on single crystals. *J Appl Phys* 59:873–879
11. Ibarra MR, Arnold Z, Algarabel PA, Morellon L, Kamarad J (1992) Effect of pressure on the magnetocrystalline anisotropy of $(\text{Er}_x\text{R}_{1-x})_2\text{Fe}_{14}\text{B}$ intermetallics. *J Phys-Condens Matter* 4:9721–9734
12. Pędziwiatr AT, Bogacz BF, Gargula R, Wróbel S (2002) Cerium influence on the spin reorientation in $\text{Er}_{2-x}\text{Ce}_x\text{Fe}_{14}\text{B}$ evidenced by Mössbauer and DSC techniques. *J Magn Magn Mater* 248:19–25
13. Pędziwiatr AT, Bogacz BF, Gargula R, Wróbel S (2002) Mössbauer and DSC studies of spin reorientations in $\text{Er}_{2-x}\text{Y}_x\text{Fe}_{14}\text{B}$. *J Alloys Compd* 336:5–10
14. Pędziwiatr AT, Wallace WE (1986) Magnetism of $\text{R}_2\text{Fe}_{14}\text{B}$ systems. *J Less-Common Metals* 126:41–51
15. Piqué C, Burriel R, Bartolomé J (1996) Spin reorientation phase transitions in $\text{R}_2\text{Fe}_{14}\text{B}$ ($\text{R} = \text{Y}, \text{Nd}, \text{Ho}, \text{Er}, \text{Tm}$) investigated by head capacity measurements. *J Magn Magn Mater* 154:71–82
16. Radwański RJ, Franse JJ (1987) Rare-earth contribution to the magnetocrystalline anisotropy energy in $\text{R}_2\text{Fe}_{14}\text{B}$. *Phys Rev B* 36:8616–8621
17. Wielgosz R, Pędziwiatr AT, Bogacz BF, Wróbel S (2000) Spin reorientation in $\text{Er}_2\text{Fe}_{14}\text{B}$ intermetallic compound. *Molecular Physics Reports* 30:167–173
18. Wolfers P, Bacmann M, Fruchart D (2001) Single crystal neutron diffraction investigations of the crystal and magnetic structures of $\text{R}_2\text{Fe}_{14}\text{B}$ ($\text{R} = \text{Y}, \text{Nd}, \text{Ho}, \text{Er}$). *J Alloys Compd* 317/318:39–43
19. Yamada M, Kato H, Yamamoto H, Nakagawa Y (1988) Crystal-field analysis of the magnetization process in a series of $\text{Nd}_2\text{Fe}_{14}\text{B}$ -type compounds. *Phys Rev B* 38:620–633